RUN-IN BEHAVIOUR AND WEAR ON HYDRAULIC PISTON SEALS – EVALUATION OF AN ENDURANCE TEST FOR PISTON ACCUMULATORS

Tobias Schulze*[,1], Vladimir Boyko[1], Michael Lenz[1], Gonzalo Barillas[2], Mert van Dawen[2], Ejnar Jørgensen[3], Erik Garde[4]

[1] *TUD Dresden University of Technology, Chair of Fluid-Mechatronic Systems (Fluidtronic), Helmholtzstrasse 7a, 01069 Dresden, Germany*
[2] *Freudenberg Sealing Technologies GmbH, Ascheröder Strasse 57, 34613 Schwalmstadt, Germany*
[3] *Lind Jensens Maskinfabrik A/S, Kroghusvej 7, 6940 Lem, Denmark*
[4] *Vestas Wind Systems A/S, Hedeager 42, 8200 Aarhus, Denmark*

* Corresponding author: Tel.: +49 351 463-42603; E-mail address: tobias.schulze2@tu-dresden.de

ABSTRACT

Hydraulic accumulators are essential components in both industrial and mobile hydraulic systems, serving various purposes from energy storage to shock absorption and energy recovery. In hydraulic pitch systems of wind turbines, piston accumulators provide significant advantages, including reliability, resilience to centrifugal forces and temperature fluctuations, as well as simple monitoring. Ensuring a proper seal between the gas and oil sides of a piston accumulator and understanding its wear characteristics are crucial for a reliable operation of the system. A precise determination of wear often requires the use of measured values.

The current paper presents the results of a 5,000-hour endurance test conducted for piston accumulators under load conditions typical for wind turbine applications and reveals insights into the run-in behaviour and wear process of the seals. During and following the test, parameters such as sealing geometry and surface roughness of inner accumulator tubes were measured. The accordance of the measured wear with Archard wear model behaviour is assessed. It could be shown that error-free sealing conditions can be expected for a period of about 20 years.

Keywords: Hydraulics, Wind Turbine, Piston Accumulator, Seal, Sealing, Surface Roughness, Wear

1. INTRODUCTION

1.1. Hydraulic systems in wind turbines

The current political requirements for CO_2 reduction make a worldwide expansion of renewable energy sources necessary [1]. This is apparent in the massive expansion of wind power plants. In the last five years alone, the global installed wind power capacity has increased by 53% to 906 GW in 2022 [2]. Wind power currently accounts for 7.3% of the world's total electricity generation, which is around 50% more than in 2018 [3].

This results in increased sales of piston accumulators, typically used in hydraulic pitch systems of wind turbines for adjusting turbine blade angles and for emergency stops to turn the blades out of the wind. However, accumulators pose a significant safety risk in turbine systems. A study of offshore turbines identified the pitch system as the most unreliable subsystem, with accumulators contributing to 10.7% of its failures [4]. Gas leakage is a major issue with hydraulic accumulators, leading to a

loss of energy storage capacity. Monitoring gas leakage in such accumulators can significantly reduce the risk, so that many signal- and model-based methods for fault detection in piston accumulators have been developed in the recent years (see e.g. [5-7]). Some manufacturers offer monitoring systems for piston accumulators, such as laser or cable position measurement systems and limit switches [8].

The piston seal therefore plays a crucial role, as the functionality of the entire wind turbine depends on it.

1.2. Piston accumulators

Hydraulic accumulators are essential components of hydraulic systems in industrial settings and mobile machinery. They find application in a wide range of scenarios. As an energy storage they take up a volume of liquid under pressure and release it again when required, for example to cover extra flow demand in case of fluctuating requirements or in the event of failure or leakage. Furthermore, they are used to reduce pressure peaks and volume flow, while also serving as a hydropneumatic spring element.

This paper investigates the sealing system and wear behaviour of a new product of piston accumulators from Lind Jensens Maskinfabrik A/S, as shown in **Figure 1**. Main parts are the gas connection (1), the tube (2), the piston (3) with piston seals and guide rings, and the oil connection (4). The accumulator was equipped with an ILR2250-100 “micro epsilon” laser measurement system (5) and a sight glass (6) to measure the position of the piston. The sealing system is composed of a polyurethane (Freudenberg 98 AU 928, hardness 98 Shore A) profile ring (*piston seal*), an NBR preload element (*energiser*), as well as gas-side and oil-side guide rings made of phenolic thermoset material. The countersurface of the sealing on the inside of the tube is a roller burnished pressure vessel steel (EN 10028) with the measured initial average roughness of $Rz = 0.758 \pm 0.095$ µm and $Ra = 0.077 \pm 0.008$ µm (see also **Figure 10**).

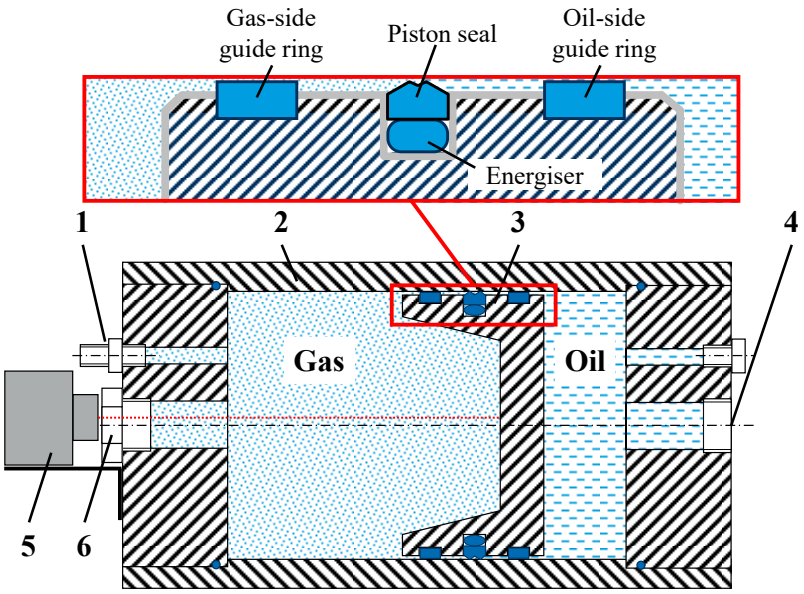

Figure 1: Schematic structure of the investigated piston accumulator

Piston-type accumulators, comprising a cylinder with a sealed, freely floating piston that separates gas (usually nitrogen) from oil, offer several advantages over bladder and membrane accumulators [9]. These advantages include the ability to operate at both high and low temperatures, and higher flow rates, resulting in higher gas compression ratios and better volume utilization rates. Additionally, manufacturing piston accumulators with various nominal volumes is particularly simple, as it can be

achieved by adjusting the tube length. In comparison to bladder and membrane accumulators, manufacturing costs of piston accumulators are relatively high. The disadvantage of piston accumulators is the high inertia of the piston, making them unsuitable for rapid charge-discharge processes. This can be partially mitigated by using lightweight materials for the pistons, such as aluminium. Within the piston accumulator, the gas and oil side are separated by the piston sealing. This imposes specific requirements on the piston seals to prevent the stick-slip effect and reduce friction, which, in turn, limits their potential application to high operating pressures. The sealing has to ensure the proper function of the accumulator throughout its whole operating life, so wear and aging of the seals need to be verified.

2. ENDURANCE TEST STAND

In order to characterise the wear behaviour of piston accumulator seals under operating conditions typical for the wind power industry and to be able to make a prediction on the expected service life of the seal, an endurance test was carried out. In total, 600,000 working cycles (corresponding to 5,000 hours of operation) were performed. The test rig consists of four individual pressure-regulated 20-liter piston accumulators (see **Figure 2, a)**) with the specifications described in **Table 1**.

The piston accumulators were mounted horizontally, which corresponds to a usual situation in a wind turbine (see **Figure 2, b)**). During operation, the oil chamber pressure p_{Oil}, the gas chamber pressure and temperature p_{Gas} and T_{Gas}, as well as the piston position of one accumulator $x_{Pis,1}$ were continuously recorded. The oil type used was the Mobil DTE 10 Excel 32. For oil conditioning and maintaining a constant operating temperature, an additional cooling circuit was included.

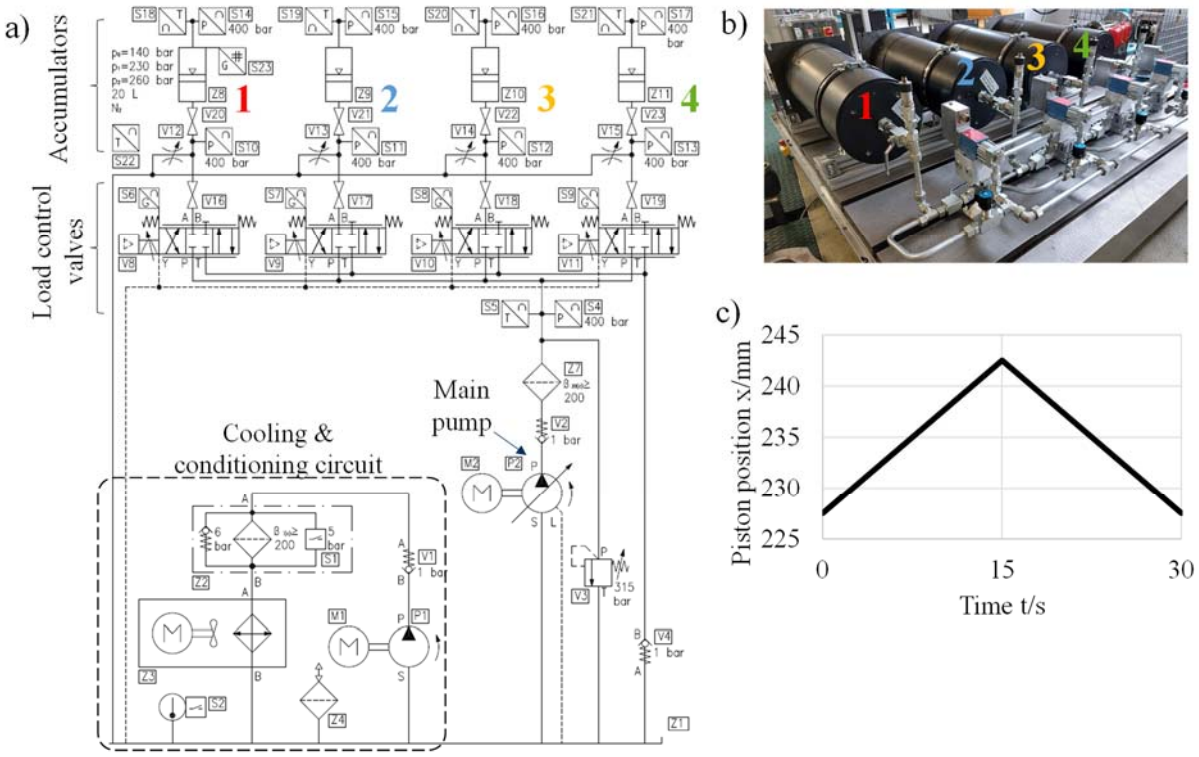

Figure 2: a) Hydraulic circuit of the test rig; b) Photo of the test rig; c) Piston target position

The piston had to maintain a central position within the accumulator, performing a 15 mm stroke from this point, as shown in **Figure 2, c**). To ensure a symmetrical load during the testing of the four cylinders, the test cycle was adjusted to a 30-second cycle with an equal volume flow for both charging and discharging.

Table 1: Geometry and operating conditions of the accumulators

Geometry/Condition	Value
Piston diameter D	240 mm
Piston stroke S	350 mm
Sliding speed $\dot{x}$	1 mm/s
Precharge pressure p_0	140 bar
Working pressure p_1 … p_2	230 … 260 bar
Oil temperature T_{Oil}	40 … 50 °C
Ambient temperature T_{Amb}	18 … 23 °C

3. EVALUATION METHOD

The wear behaviour of the accumulator was mainly determined by measuring the geometry of the piston seal, the surface roughness of the tube and by evaluating the measured process values of the test stand. All four accumulators were disassembled at intervals of 200,000 cycles for measurements of seal geometry and inner tube surface roughness. Following each measurement, the pistons were reinstalled in their original orientation to avoid any rotational variability. To determine the run-in behaviour, additional measurements were conducted at accumulator 1 after 1,500, 3,000 and 4,500 cycles (resp. 12.5, 25 and 37.5 hours of operation).

The process values were recorded for each 100th cycle, evaluated according to their absolute or average value and compared throughout the 600,000 cycles. In particular, the following values were evaluated:

Table 2: Evaluated process values of the test stand

Process value	Description
Precharge pressure	Before each disassembly process, the precharge pressure of the nitrogen was documented and compared to the value from the previous start-up
Piston position	The absolute position of the piston was measured with a laser measurement system. A change of the piston position would indicate gas leakage.
Pressure difference (gas and oil side)	The pressure on the gas and oil side of each accumulator was measured; their difference is an indicator for changing friction forces that might be caused by increased wear on the sealing setup of the piston
Temperature	Oil- and gas temperature were measured at each accumulator in order to monitor and evaluate temperature influences

To determine changes in the seal geometry, several geometrical measurements were taken. The cross section height and width of the piston seals, energisers, and guide rings were measured with a micrometer (resolution: 10 µm, error: 4 µm) at 12 points around the section (0°, 30°, 60° … 330°) after each test stage following the manufacturer's markings on the seals in order to ensure a high degree of reproducibility of the measurement. Additionally, the cross section profile of the sealing was measured with a profilometer Keyence VR-6000 (error: 4 µm). The weight of the seals and guide rings was measured with an analytical balance scale (Kern ABT 120 scale, linearity ±0.2 mg). The seal's inner diameter was determined using an 8-point assessment with a DMG DMU Eco80 linear CNC-machine. All values were determined in the dismantled, unstressed state with oil removed from the surface. **Figure 3** provides an overview of the seal setup at the piston and the measured variables.

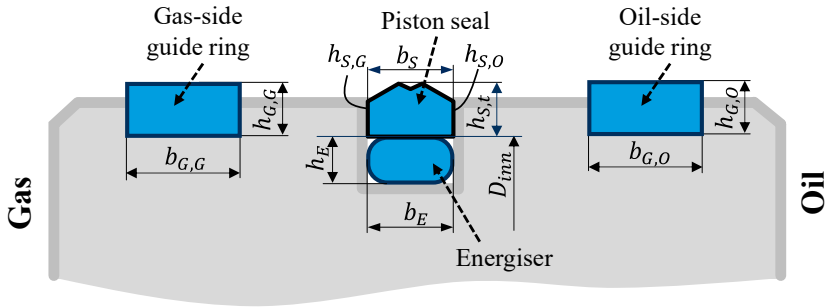

Figure 3: Seal setup and measured geometrical values

To give a brief insight into the measurement procedure and the occurring deviations, **Table 3** shows the measurements for the piston seal height at accumulator 1 after 400,000 cycles. It can be seen that the standard deviation of the micrometer measurements is 17 µm. In order to reduce the influence of random measurement errors, all further evaluation of geometric dimensions is based on the mean value of all 12 measuring points. The results are verified through additional measurement with the profilometer. It shows the decrease in the cross section height (compared to a factory-new piston seal) with a much lower standard deviation of 3.4 µm.

Table 3: Measurements for piston seal at accumulator 1 after 400,000 cycles

Micrometer		Profilometer	
Measurement point	Total height h_t	Measurement point	Decrease in total height Δh_t
0°	4.030	0°	0.079
30°	4.020		
60°	4.025	60°	0.082
90°	4.000		
120°	4.005	120°	0.084
150°	4.010		
180°	4.015	180°	0.084
210°	3.985		
240°	3.980	240°	0.074
270°	3.985		
300°	3.990	300°	0.077
330°	4.020		
Mean value $\bar{h}_t$	4.005	Mean value $\overline{\Delta h_t}$	0.080
Std. deviation σ	0.0170	Std. deviation σ	0.0034

4. RESULTS

4.1. Run-in process

The factory-new sealing setup on the piston is expected to show a run-in process during the first operating hours, with increased wear and more rapidly changing process values, until the friction couples between the seal, guide ring, and tube have developed their individual stabilized friction state. Therefore, especially the measured cross section height of the sealing lips is expected to decrease more rapidly during these first operating hours.

To prove this assumption and determine the required time for the run-in process, additional measurements on accumulator 1 were conducted during the beginning of the experiments after 1,500,

3,000, and 4,500 cycles. **Figure 4** shows the width, total cross section height, and mass of the piston seal of accumulator 1. It can be seen that after 1,500 cycles (equivalent to 12.5 hours of operation), the run-in process is mostly completed, as there are only minor changes in the geometrical measurements. Changes in the cross section width show an increase by 18 µm after 1,500 cycles (20 µm after 3,000 cycles, 22 µm after 4,500 cycles respectively). The total cross section height h_t decreased by 63 µm after 1,500 cycles (66 µm after 3,000 cycles, 75 µm after 4,500 cycles respectively). The mass of the sealing increases by 48 mg after 1.500 cycles (53 mg after 3,000 cycles, 62 mg after 4,500 cycles respectively), which is attributed to swelling overlaying a possible reduction due to abrasive wear. These values are confirmed by further measurements after 200,000, 400,000 and 600,000 cycles, as the further changes are small.

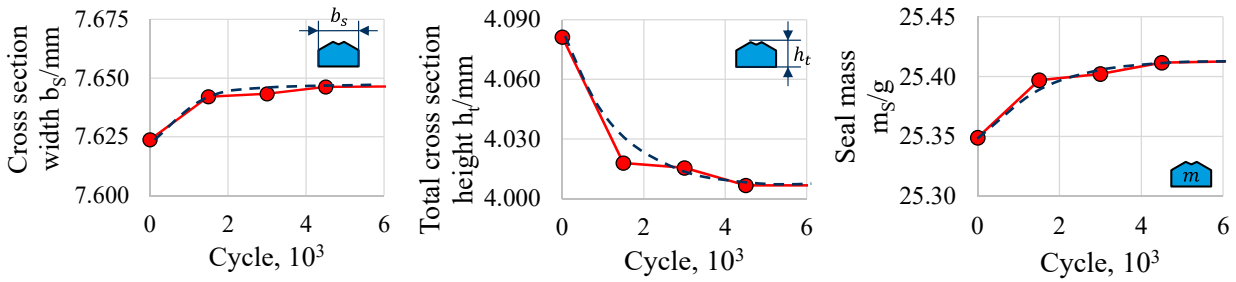

Figure 4: Evaluation of the run-in process at accumulator 1

4.2. Characterization of friction

An additional value to evaluate the stabilized friction couple on the seal is the resulting pressure difference between gas and oil side of the seal $p_\mathrm{d} = p_\mathrm{Oil} - p_\mathrm{Gas}$. Given that no other forces are acting on the piston and inertia forces are minimal, p_d is proportional to the frictional force F_fr acting on the sealing system. The comparison between different cycles provides an indicator for changing friction properties over the course of the experiment, as the trajectory is controlled to remain uniform. **Figure 5** shows the measurement results for accumulator 1 for cycle 201,000. It presents the measured piston trajectory (actual distance from the laser measurement system to the piston, see position '5' in **Figure 1**), the gas pressure p_Gas, gas temperature T_Gas, as well as p_d. The pressure difference shows a characteristic curve with a slight increase throughout the piston movement and a sign change when the piston reverses.

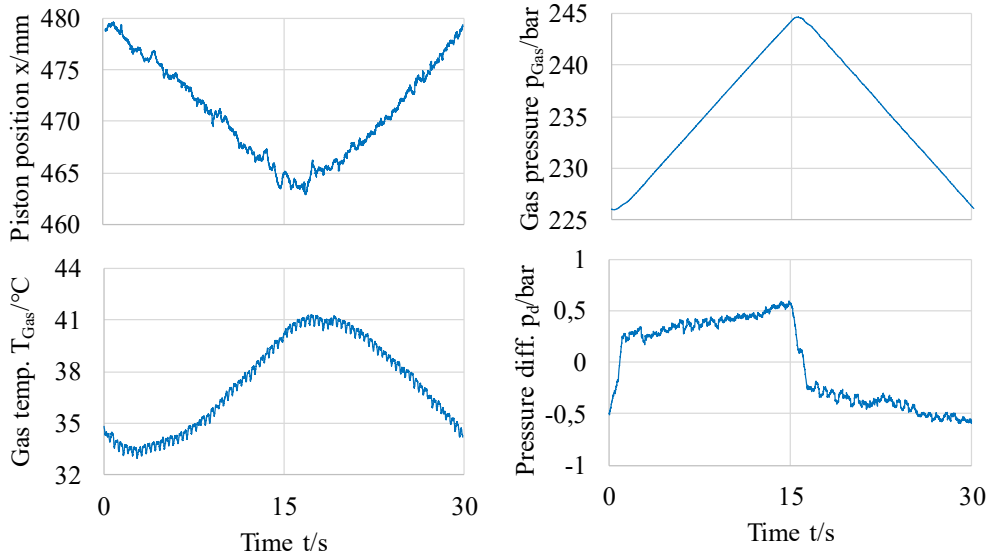

Figure 5: Measurements for cycle 201,000 at accumulator 1

For the presented measurements at cycle 201,000, it is assumed that the run-in-process is completed and the friction couple has been fully stabilized. However, at cycle 200,000, the seal was inspected for wear, which involved full dis- and reassembly. Comparing the values of the pressure difference p_d throughout all cycles, it was observed that after each reassembly p_d reaches significantly higher values as compared to immediately before inspection.

Figure 6 compares the pressure difference in all accumulators shortly after the inspection events and again after additional 100,000 cycles. Inspections of all accumulators were carried out after 4,500, 200,000, 400,000 and 600,000 cycles. The figure shows that shortly after reassembly (displayed in red colours) a higher value of pressure difference was measured in most cases. Each accumulator shows a characteristic shape for the course of the pressure difference throughout the respective cycle shortly after reassembly. The stabilized state after additional 100,000 cycles (displayed in blue colours) is constant throughout the different cycles and repeats over the reassembly events.

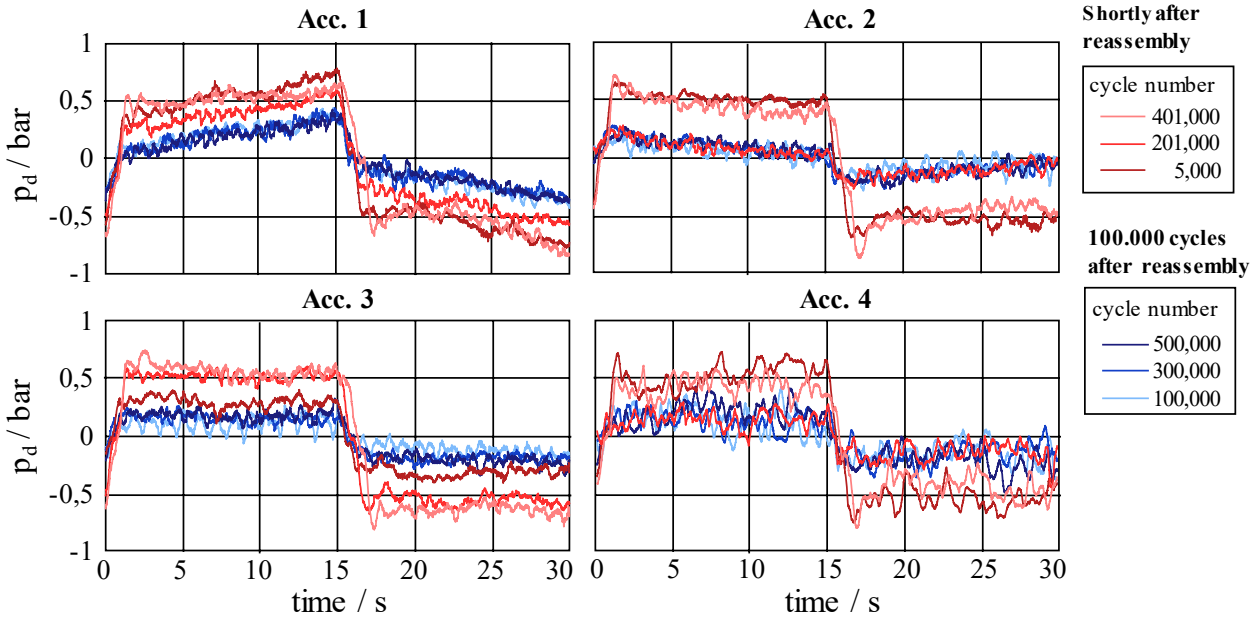

Figure 6: Pressure difference in accumulators shortly after inspection and after stabilization

4.3. Precharge pressure

To evaluate the potential internal and external leakage of the working gas and hydraulic oil, the precharge pressure change before and after the last 200,000 cycles was measured at the same gas temperature of T_{Gas} = 19.5 °C. A slight increase in precharge pressure by 0.25% on average could be observed, indicating a minor internal oil leak from oil side to gas side. Applying the isothermal equation of state for ideal gases, the permeated oil volume can be estimated at 40 ml.

Table 4: Precharge pressure changes in the last test stage (400,000 to 600,000 cycles)

Parameter	Acc. 1	Acc. 2	Acc. 3	Acc. 4
Start precharge pressure $p_{0,400}$/bar	140.25	140.31	140.20	140.14
End precharge pressure $p_{0,600}$/bar	140.54	140.66	140.51	140.45

Since a visual inspection of the accumulators after disassembling did not reveal significant traces of oil, the measured increase can also be partially attributed to the inaccuracy of the pressure sensors. No oil mist could be observed while draining the gas.

4.4. Changes in the sealing

From the measurement results of the piston seal presented in **Figure 7**, a noticeable change in the cross section height is evident, which can be attributed to the initial run-in process. After approximately 4,500 cycles, the seal height continued to gradually decrease at a notably diminished rate. The height on the oil side showed a faster decline compared to the gas side (0.44% average reduction vs. 0.27% on the gas side), presumably attributable to chemical reactions occurring due to contact with the oil, thus accelerating the wear. The total height reduction after 600,000 cycles amounted to 0.06 mm or 0.32%.

Regarding the sealing width, it exhibited an initial increase during the first 200,000 cycles and subsequently reached a near-constant state, showing minimal variation. Even after 600,000 cycles, the width increase remained below 0.05 mm. The sealing weight also showed a similar pattern, increasing during the first test stage due to oil impregnation and remaining nearly constant after 200,000 cycles. The total weight increase after 600,000 cycles is estimated at 0.2 g. The inner diameter of the seals underwent a reduction following the run-in period and subsequently changed within a range of 0.1 mm.

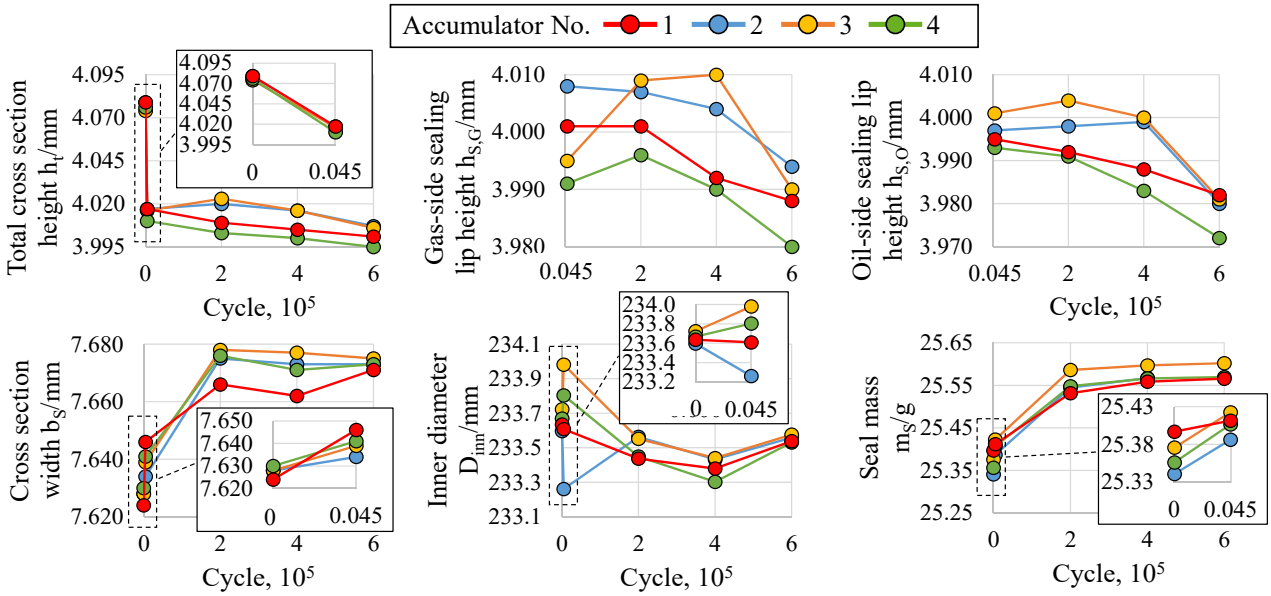

Figure 7: Measurement results of the piston seal

Estimating the remaining service life based on available data can be challenging and requires further studies, such as accelerated life-time tests to determine wear. However, by assuming a critical seal height change of 12% (manufacturer specification), after which a gas leakage becomes likely, and extrapolating the total cross section height h_t in **Figure 7** linearly, the remaining service life can be estimated to be approximately 20 years.

In addition to the manual measurement of the sealing lip height, a profilometer Keyence VR-6000 was used to determine the cross section profile of the piston sealing. The profile shows wear on the sealing lips with rounder edges compared to the factory new and unused profile (see **Figure 8**). By evaluating the depth of the groove between both sealing lips, the measurements shown in **Figure 7** are confirmed and a reduced sealing height of about 0.08 mm after 600,000 cycles was measured. This measurement verifies the previous values measured with the micrometer which also determined a decrease by 0.08 mm.

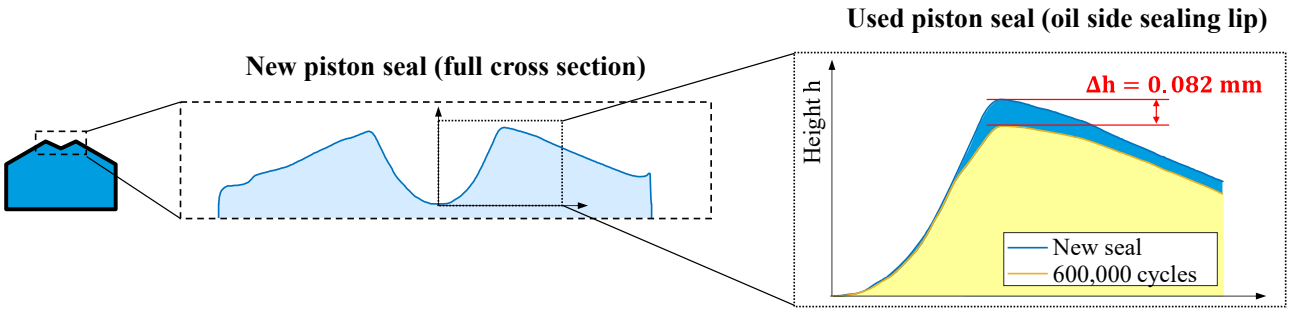

Figure 8: Cross section of the sealing lips and evaluated groove depth

Both oil-side and gas-side guide rings experienced a decrease in height and width (s. **Figure 9**). Similar to the seal ring, the deformation of the guide ring on the oil side was more pronounced compared to the gas side. On average, the height of the oil-side guide ring decreased by 1.77%, while the gas-side guide ring exhibited a slightly lower average height decrease of 1.19%. This difference may also be due to measurement inaccuracies. The mass of the oil-side guide ring showed a significant increase, approximately 1.26% higher than the gas-side ring, which could also potentially be attributed to the oil absorption.

The measurements performed on the energiser of the accumulator 1 did not detect any changes in the geometry.

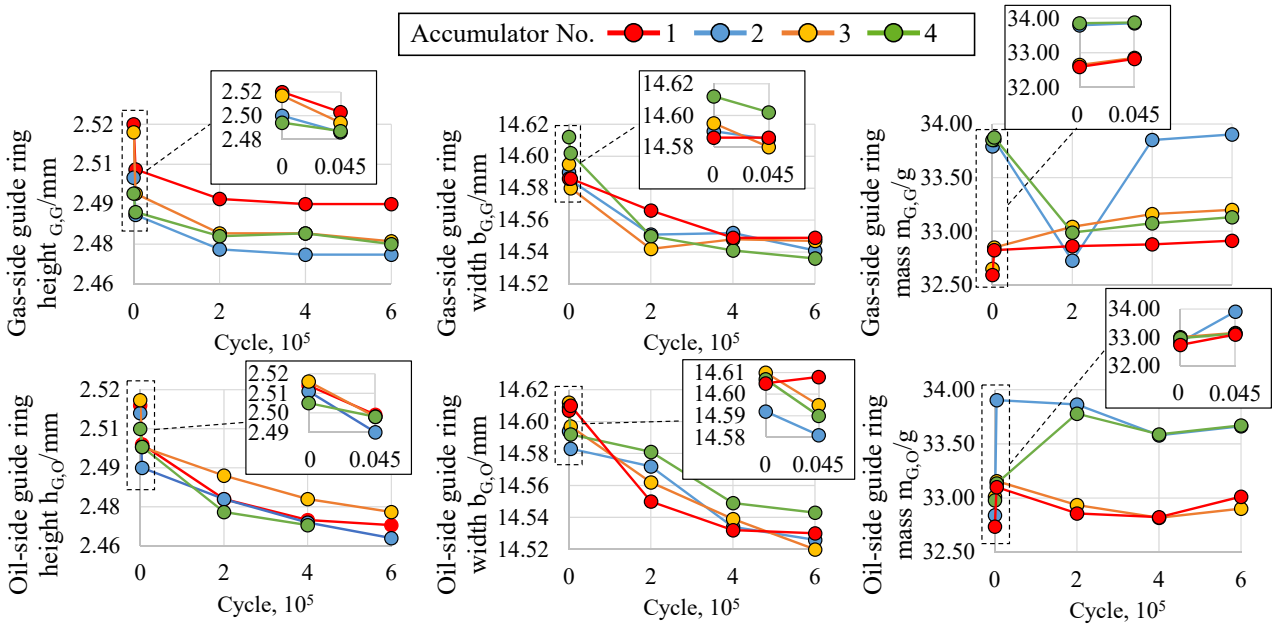

Figure 9: Measurement results of the gas-side (upper row) and oil-side (lower row) guide ring

4.5. Roughness of the inner tube surface

In addition to measuring the seal geometry, the roughness values *Ra* and *Rz* of the inner surface of the accumulators in the area of the piston movement were measured. These measurements were taken every 200,000 cycles using a profilometer MahrSurf PS10 at four points around the circumference. Furthermore, the full peak height *Rpkx*, the kernel roughness depth *Rk*, and the full valley depth *Rvkx* were determined for the accumulator 1 before and after the test. **Figure 10** demonstrates the change in the roughness values over the entire duration of the experiment.

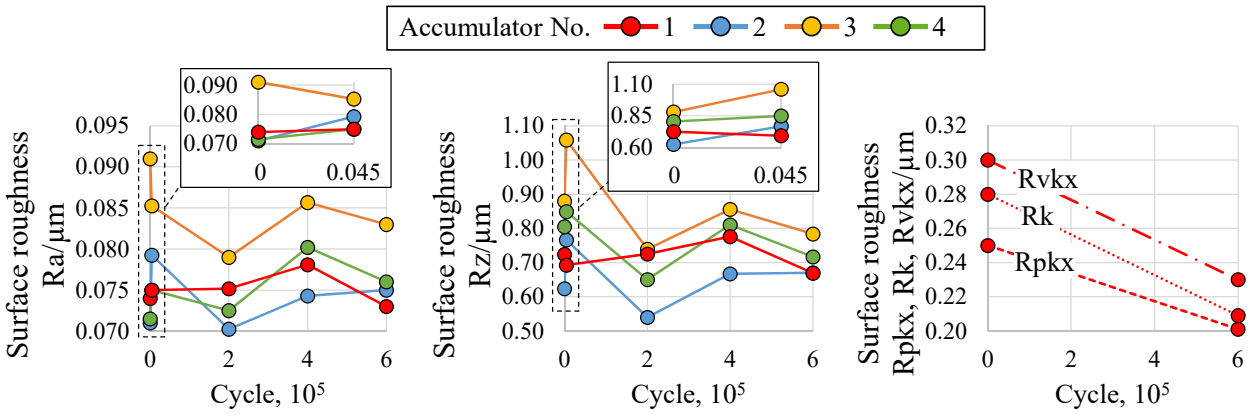

Figure 10: Change in surface roughness over the test period

No significant reduction during the test can be read from the usual values *Ra* and *Rz*. The fluctuations in the value are attributable to the measurement deviations of the instrument. However, a significant reduction in the peak, kernel, and valley depth can be observed, indicating the run-in and polishing effect.

5. WEAR EVALUATION AND LIFETIME PREDICTION

The observed evolution of cross section wear is assessed by means of a simplified Archard [10] wear model. The regular Archard model predicts the volume of material lost to wear V_W with the equation

$$V_{\mathrm{W,A}} = k \int \frac{F_\mathrm{N}}{H} \mathrm{d}s, \tag{1}$$

F_N being the normal force acting in the contact, s the sliding distance between the friction partners, H the hardness of the softer material, and k an empirical constant.

While the literature reports a limited applicability of the Archard model for elastomer friction on hard surfaces, a variety of more elaborate models for elastomer wear, often modifications of the Archard model, have been proposed to overcome its shortcomings – see e.g. [12] for a non-comprehensive overview. These studies are typically concerned with deriving general models for predictive simulation in the context of elastohydrodynamics (EHD). For this experimental assessment, the original model's simplicity is considered favourable. This is because micromechanical processes are not observable, and typical model parameters such as sliding velocity and load are kept constant in the experimental setup. Therefore, parameters of refined models are either inaccessible or irrelevant. Model simplicity should also be considered in relation to its potential application in a condition monitoring context, where extensive parameter identification may not be feasible and a limited number of signals must suffice.

A proportional friction law $F_\mathrm{fr} \propto F_\mathrm{N}$ is assumed, since the sliding velocity as a further parameter is kept constant during the experiment. The influence of variations in temperature, which was controlled to stay constant, is neglected. With furthermore constant hardness H, and observing $p_\mathrm{d} \propto F_\mathrm{fr}$ as stated in Section 4.1, the model reduces to an expression

$$V_\mathrm{W} = K \int p_\mathrm{d} \, \mathrm{d}s \tag{2}$$

The result is an abstracted model postulating wear volume as proportional to friction work.

Since the sliding distance was not measured directly for all four accumulators, it is derived from p_Gas by supposing ideal gas behaviour such that

$$s = \frac{s_0 p_{\mathrm{Gas},0}}{T_{\mathrm{Gas},0}} \cdot \frac{T_{\mathrm{Gas}}}{p_{\mathrm{Gas}}}, \tag{3}$$

where 0 denotes the state variables at the moment of initial charging of the accumulators, and s is measured from the rear wall of the cylindrical gas volume.

The evaluation of the integral V_{W} with as yet unknown constant K is shown in **Figure 11**. The values are broadly comparable between the accumulators, although accumulator 2 has the markedly lowest. The figure highlights the inspection events at 4,500 and 200,000 cycles. As reported in Section 4.2, the pressure difference tends to increase clearly after inspections, leading to an increased value of the per-cycle integral. **Figure 11** shows how this comparatively high value stabilizes or decreases only slowly over a couple 1,000 to up to several tens of thousands cycles (between a few hours to several days of operation) and then changes rather abruptly back to a value that is similar to the previously stabilized friction state before the disassembly. This indicates a sudden change towards a more favourable tribological regime and is observed for all four accumulators for each inspection with exception of accumulator 3, at 4,500 cycles, where the value is lower after inspection, and accumulators 2 and 4 at 200,000 cycles, where a higher value appears right after disassembly but decreases more rapidly. The number of cycles for stabilizing differs between the accumulators and appears to be random, indicating a spontaneous transition between the stable tribological regimes.

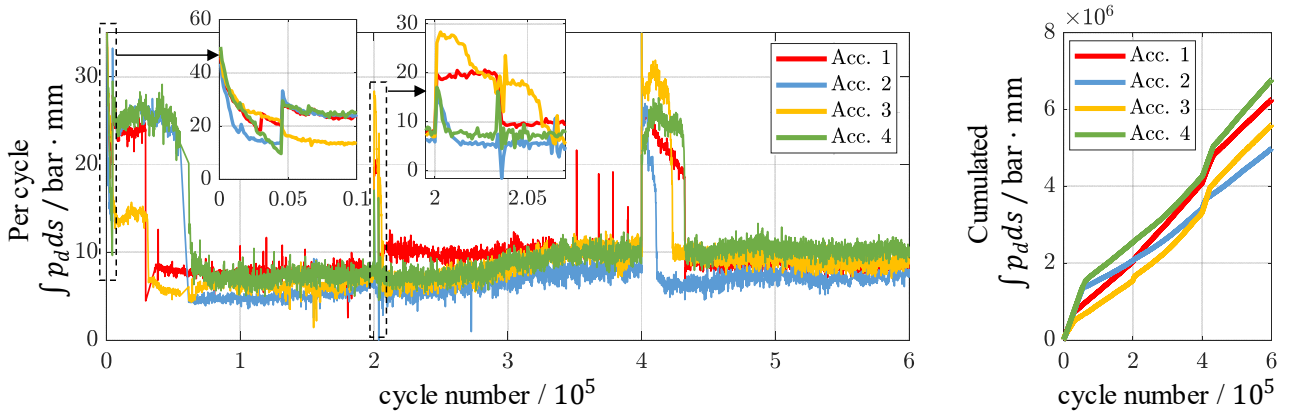

Figure 11: Evaluation of wear integral

The representation of the per-cycle wear integral confirms the spontaneous change towards a much lower value after about 1,000 up to 10,000 cycles after inspection. Due to its diverse influencing factors, this behaviour can unfortunately not be discussed in further detail within the limited space of this publication.

During the favourable equilibrium, the per-cycle integral, which according to the models is a measure for wear, is markedly highest for accumulator 1, in particular after the inspection at 200,000 cycles. Accumulators 3 and 4 exhibit comparable rates during those periods, while it is notably lower for accumulator 2. During the periods of increased per-cycle value immediately after inspections, the accumulated integral increases much faster, and in particular the phases after the first and the third inspection contribute significantly to the overall value of the wear measure attained during the test.

In **Figure 12**, the computed wear integral is exemplarily depicted in relation to the observed changes in the sealing lip height presented in **Figure 7**. The wear model according to Equation (2) would postulate a linear dependency, with the same slopes K for all test specimens for each of the wear locations.

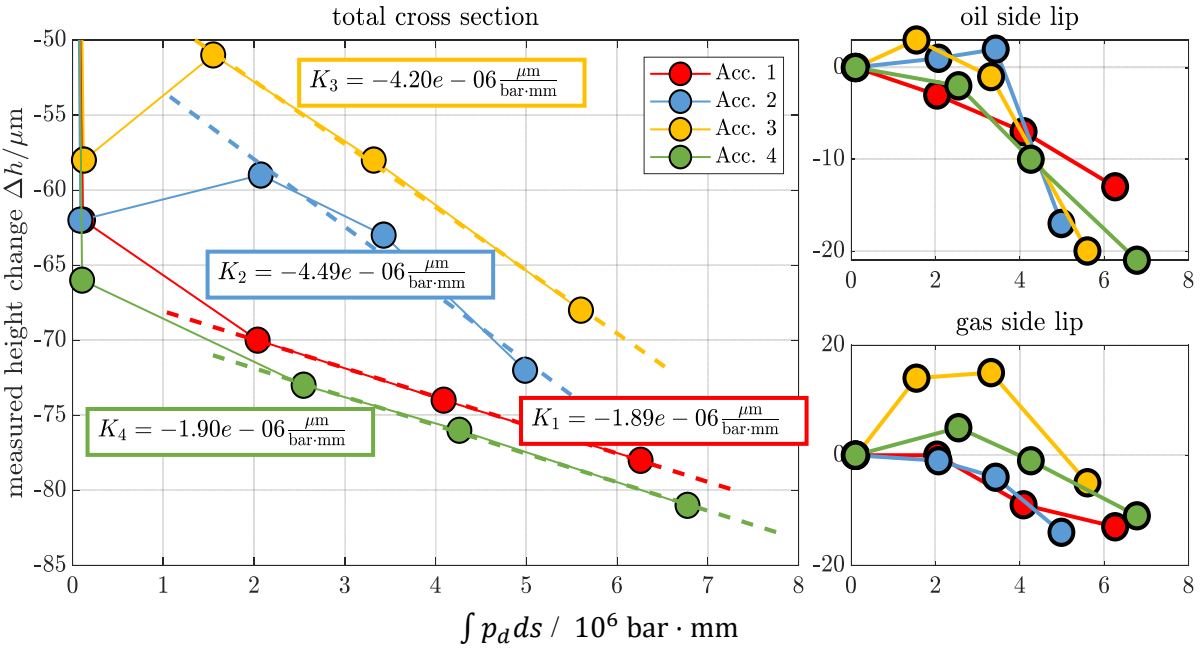

Figure 12: Wear integral vs. observed wear

The presented results cannot be interpreted to support this on a global level for neither of the wear locations discussed here. Possible explanations are:

a) the model being overly simplistic and hence inapplicable for the tribological system;

b) as discussed in Section 4.4, the quantitative assessment of the sealing wear during the tests is complicated by the superposition of wear and swelling, and by the low total amount of observed wear and associated measurement error. The resulting uncertainties complicate the model assessment;

c) the measured cross section and sealing lip heights being imperfect proxies for the volume of worn material from Equation (3), the quality of which could not be comprehensively assessed over the experiment; however **Figure 8** gives an indication.

The total cross section diagram does indicate a partial relation between the model and the measured results for the higher cycle numbers. If only the data points pertaining to the inspections at 200,000, 400,000 and 600,000 cycles are considered, linear fits of high significance, with values of $R^2 = 0.9997$, 0.9686, 0.9992 and 0.9988 for the four accumulators respectively, are achieved. There is a striking accordance of the slopes for accumulators 1 and 4, and those for 2 and 3. A possible interpretation is the model failing for the run-in process up to the 200,000 cycles inspection, at which point the wear process has stabilized sufficiently for the model to capture its evolution. The two different slopes may be explained by accumulators 2 and 3 having undergone swelling during the initial phase of the experiment to an increased degree, to the point where the cross section height increased during operation despite wear. In this interpretation, two distinct friction pairings have formed, with different associated wear constants K. It is acknowledged that more data points for each accumulator would be desirable in order to allow for a confident statement regarding the model's suitability for the later phase of the experiment, which at this point must remain speculative to a degree. The graphs for the two single sealing lip heights do not show a similar indication of partial accordance with the model. However, as stated in Section 4, the associated measurements are associated with higher uncertainty. Further tests with higher cycle numbers for a larger, more significant quantity of observed wear, as well as a revised experimental setup in order to exclude uncertainties, could provide a basis to confidently evaluate the applicability of the model or find a

suitable alternative. This is, however, of limited feasibility considering the required high cycle counts, and motivates an accelerated testing scheme.

6. CONCLUSION AND OUTLOOK

The conducted experiments deliver results for wear in piston accumulators on the example of an application-driven test cycle. It was shown that the run-in process of the sealing is completed after only few cycles and about 12 hours of operation. Extensive measurements of the sealing geometry confirm a safe operation of the piston accumulator throughout its desired live cycle.

The wear models according to Holm-Archard and Fleischer were applied to the measurements. The evolution of the wear integral indicates a wear intensive tribological regime after assembly, including after inspections, which after several thousands to tens of thousands of cycles changes spontaneously to a stable, more favourable regime. With the available experimental results, only a limited assessment of the model applicability is possible. It clearly fails during the early stages of the experiment. The wear measure of total cross section height appears to follow the model behaviour for higher cycle numbers > 200,000, but the available amount of data points, together with measurement uncertainties, make a verdict difficult.

While extended tests would be desirable to fully assess the evolution of wear in the component, the long cycle times lead to a prohibitively long duration. This motivates the design of an accelerated test procedure. To provide meaningful results for the component under its operation conditions, such tests must preserve a comparable tribological regime, characterized by the Hersey number and the dynamic stiffness of the sealing material, which both depend on the sliding velocity in the contact. An increase in velocity could be compensated by targeted control of temperature – and hence viscosity – and pressure, so as to maintain both quantities in the same range as under operating conditions.

NOMENCLATURE

Symbols

b	Cross section width	mm
D	Diameter	mm
e^*	Energy density of the tribological system	J
F	Force	N
h	Cross section height	mm
H	Material hardness of the softer friction partner	-
k	Empirical wear coefficient	-
m	Mass	g
p	Pressure	bar
Ra	Average roughness	µm
Rk	Kernel roughness depth	µm
$Rpkx$	Full peak height	µm
$Rvkx$	Full valley depth	µm
Rz	Ten-point mean roughness	µm
S	Piston stroke	mm
T	Temperature	°C
V	Volume	l
W	Wear volume	mm^3
x	Piston position	mm

Indexes and Abbreviations

0	Initial/precharge state
1	Minimum working pressure
2	Maximum working pressure
d	Difference between oil- and gas-side
fr	Friction force
G,G	Gas-side guide ring
G,O	Oil-side guide ring
Gas	Gas side
Inn	Inner diameter
N	Normal force
Oil	Oil side
S	Piston seal
S,G	Gas-side sealing lip
S,O	Oil-side sealing lip
t	Total

REFERENCES

[1] European Commission (2020) Stepping up Europe's 2030 climate ambition. Investing in a climate-neutral future for the benefit of our people, COM/2020/562

[2] Statista Research Department (2023) Cumulative installed wind power capacity worldwide from 2001 to 2022, online: https://www.statista.com/statistics/268363/installed-wind-power-capacity-worldwide/ (accessed on 15 October 2023)

[3] Statista Research Department (2023) Share of electricity generation from wind energy sources worldwide from 2010 to 2022, online: https://www.statista.com/statistics/1302053/global-wind-energy-share-electricity-mix/ (accessed on 15 October 2023)

[4] Carroll J, McDonald A, McMillan D (2015) Failure rate, repair time and unscheduled O&M cost analysis of offshore wind turbines. Wind Energy, pp. 1107-1119

[5] Pfeffer A, Glück T, Kemmetmüller W, Kugi A (2015) State of charge estimator design for a gas charged hydraulic accumulator. Journal of Dynamic Systems, Measurement and Control, 137(6)

[6] Liniger J, Soltani M, Pedersen H C, Carrol J, Sepehri N (2017) Reliability based design of fluid power pitch systems for wind turbines. Wind Energy, 20(6), June, pp. 1097-1110

[7] Liniger J, Sepheri N, Soltani M, Pedersen H C (2017) Signal-based gas leakage detection for fluid power accumulators in wind turbines. Energies, 10(3), Mar., pp. 1-18

[8] Hydac International (2023) Accumulator Technology. Product Catalogue EN 3.000.18/04.21

[9] Gebhardt N, Weber J (2020) Hydraulik – Fluid-Mechatronik. Springer, Berlin

[10] Archard J (1953) Contact and rubbing of flat surfaces. Journal of applied physics, 24(8), pp. 981-988

[11] Hakami F, Pramanik A, Basak A K, Ridgway N (2019) Elastomers' wear: comparison of theory with experiment. Tribology International, pp. 46-54.